

Observation of Long-Radial-Range-Correlation in Turbulence in High-Collisionality High-Confinement Fusion Plasmas

R. Hong,¹ T. L. Rhodes,¹ P. H. Diamond,² Y. Ren,³ L. Zeng,¹ X. Jian,⁴ K. Barada,¹ G. Wang,¹ and W. A. Peebles¹

¹*Physics and Astronomy Department, University of California, Los Angeles, CA 90095, USA*

²*Center for Astrophysics and Space Sciences, University of California, San Diego, La Jolla, CA 92093, USA*

³*Princeton Plasma Physics Laboratory, Princeton, NJ 08543, USA*

⁴*Center for Energy Research, University of California, San Diego, La Jolla, CA 92093, USA*

We report on the observation of spatially asymmetric turbulent structures with a long radial correlation length in the core of high-collisionality *H*-mode plasmas on DIII-D tokamak. These turbulent structures develop from shorter wavelength turbulence and have a radially elongated structure. The envelope of turbulence spans a broad radial range in the mid-radius region, leading to streamer-like transport events. The underlying turbulence is featured by intermittency, long-term memory effect, and the characteristic spectrum of self-organized criticality. The amplitude and the radial scale increase substantially when the shearing rate of the mean flow is reduced below the turbulent scattering rate. The enhanced LRRC transport events are accompanied by apparent degradation of normalized energy confinement time. These findings constitute the first experimental observation of long-radial-range turbulent transport events in high-collisionality *H*-mode plasmas, and demonstrate the role of mean shear flows in the regulation of turbulence with long-radial-range correlation.

The classic approach of describing transport and relaxation adopts the Chapman-Enskog theory and presumes a clear separation of scales between fluctuations and macroscopic systems. However, long-range correlation can develop and act to drive scale-invariant evolution. The long-range correlation events can be intermittent, as in avalanches in self-organized criticality, or coherent, as in large-eddy circulation. Such transport events have been observed in incompressible fluids [1], plasmas [2], neural activities [3], complex networks [4], phase transitions [5], etc. In any of those cases, the key issues are the characterization of long-range events and the understanding of their origins.

The long-range correlation is also highly relevant to studies of magnetic fusion energy. One major challenge for fusion plasma physics is to predict and control turbulence and transport. The conventional turbulent transport model is based on a set of local expressions of flux-gradient relations [6]. However, there are several indications that the local model is inadequate [7]. One of the most prominent examples is the breakdown of gyro-Bohm scaling that is a fundamental element of the local approach [6, 8]. Such a departure implies that the radial scales of turbulent structures in fusion plasmas are likely in excess of the expected turbulence cell size. That is, turbulent structures with a long-radial-range correlation (LRRC) may exist in fusion plasmas.

In fusion plasmas, turbulent structures with LRRC have been predicted by theory and simulations, including avalanches [9], turbulence spreading [10], streamers [11], etc. There are some experimental observations for such structures from low-confinement mode (*L*-mode) discharges [12–16]. However, until now, it remains an open question whether such LRRC mode can occur in the high-confinement mode (*H*-mode), which is the preferred operation scenario for ITER and fusion reactors. In addition, substantial degradation of plasma confinement in the *H*-mode discharges has been widely observed when the collisionality is raised [17] or the averaged density approaches the Greenwald density [6]. Further analyses found that, as

collisionality is increased, the core electron thermal diffusivity increases substantially, while the ion thermal diffusivity is similar [18–20]. It is an indication that core turbulent transport in the electron channel, due to an increase in intensity or the radial scale, plays an important role in the confinement degradation. Therefore, it is of practical importance and interest to identify and characterize core turbulence and their correlations that emerge in high-collisionality or high-density *H*-mode fusion plasmas.

In this letter, we show that shorter wavelength turbulence develops into spatially asymmetric turbulent structures with a long-radial-range correlation in the mid-radius region of high-collisionality *H*-mode plasmas on the DIII-D tokamak. The magnitude and the radial scale of those turbulent structures increase significantly when the $E_r \times B$ mean flow shearing rate decreases. These findings thus provide the first experimental evidence for the existence of the LRRC turbulent structures and resulting transport events in *H*-mode plasmas at high collisionality, as well as the potential role of the radially sheared $E_r \times B$ mean flow in regulating the long-range transport dynamics. The emergence of such LRRC transport events may serve as a candidate explanation for the degrading nature of *H*-mode core plasma confinement at high-collisionality.

The experiments were performed using upper single-null plasmas with closed divertors on the DIII-D tokamak [21]. A dimensionless collisionality scan was performed by varying the toroidal magnetic field B_t and the plasma current I_p by a factor of 1.6 with fixed B_t/I_p , which is a standard approach used in previous dimensionless scan experiments on DIII-D [18]. In these discharges, the collisionality ($\nu_e^* \sim n_e/T_e^2$) is scanned, with well-matched plasma density, n_e , and some transport-relevant dimensionless parameters in the mid-radius region, e.g., ρ^* (ratio of ion gyro-radius to plasma minor radius ρ_i/a), $\beta_N = \frac{\beta}{I/aB_t}$ (normalized ratio of plasma to magnetic pressure), q (safety factor), T_e/T_i (electron-to-ion temperature ratio), κ (elongation), δ (triangularity). The neutral beam injection of $P_{\text{NBI}} = 7$ MW provides constant input torque and heating power

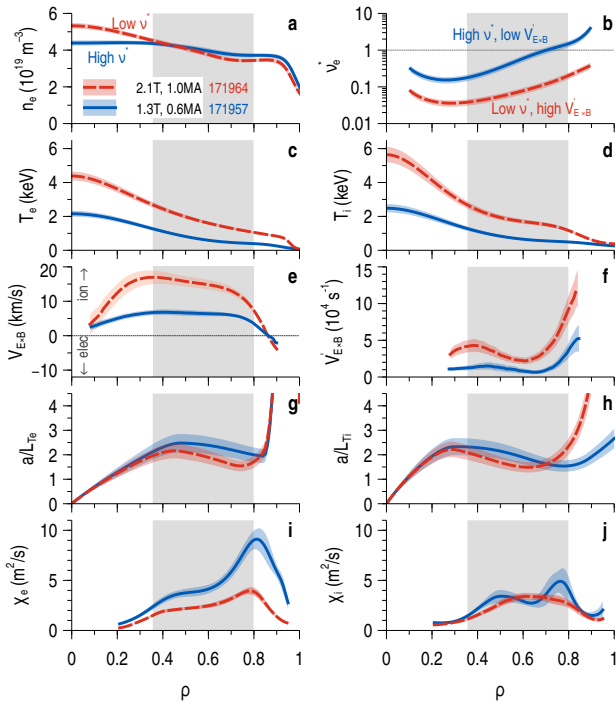


Figure 1. Radial profiles of (a) the electron density, (b) the electron collisionality, (c) the electron temperature, (c) the ion temperature, (e) the mean $E_r \times B$ shear flow, (f) the mean flow shearing rate, (g) the normalized electron temperature gradient, (h) the normalized ion temperature gradient, (i) effective electron thermal diffusivity, and (j) effective ion thermal diffusivity. The blue curves represent profiles from a high collisionality discharge, and the red curves corresponds to those in a low collisionality shot. Gray shadings indicate the region of interest in this study.

in each shot. Large-scale magnetohydrodynamics (MHD) instabilities are mitigated and of similar amplitude ($\tilde{B}_\theta < 0.1$ mT) in these shots. The line-averaged plasma density is $\bar{n}_e = 4 - 4.2 \times 10^{19} \text{ m}^{-3}$ in these discharges. The corresponding Greenwald fraction is raised from about 0.5 to 0.9. Note that the pedestal conditions and edge localized modes (ELMs) characteristics changed dramatically during the collisionality scan. To avoid confusion, the analysis presented in this study is focused on the profiles and fluctuations between ELMs. The electron density and temperature profiles are measured using Thomson scattering diagnostics [22]. The profiles of carbon ion density, temperature, and velocities are measured by the charge exchange recombination (CER) diagnostic system [23]. These carbon ion profiles are used to infer the mean $E_r \times B$ shear flow using the ion force balance equation [24]. The multi-channel Doppler backscattering (DBS) diagnostics [25] are used to detect the electron density fluctuations at the wavenumber range of $5 < k_\perp < 10 \text{ cm}^{-1}$ ($1 < k_\perp \rho_s < 4$ where ρ_s is the ion gyro-radius with sound speed) in the mid-radius region ($0.35 < \rho < 0.8$ with ρ the normalized minor radius).

Figure 1 shows the relevant radial profiles at two distinct values of the collisionality. The low collisionality discharge has a more peaked density profile (Figure 1(a)), consistent

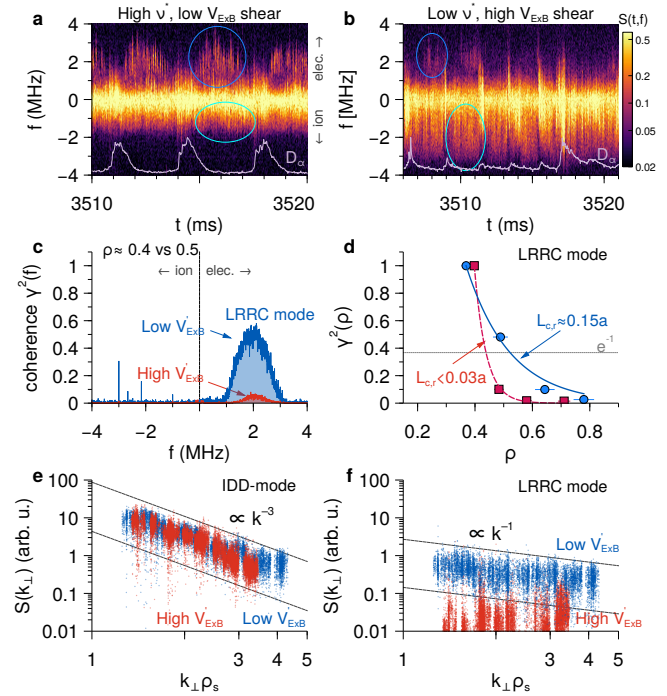


Figure 2. First row: spectrogram of density fluctuations measured by the DBS diagnostics at $\rho \approx 0.5$ in high collisionality (a) and low collisionality (b) discharges, respectively. Here, the ELM evolutions are indicated by the D_α emission intensity (gray curves). Second row: (c) Coherence between local density fluctuations at $\rho \approx 0.4$ and 0.5 ; (d) Radial profiles of the peak cross-coherence for the LRRC turbulence, where the channel at $\rho_0 \approx 0.4$ is chosen as the reference. The curves represent the exponential fits, i.e., $\gamma^2(\rho) = \exp(-\frac{\rho-\rho_0}{L_{c,r}})$, where $L_{c,r}$ represents the radial correlation length in terms of the minor radius. Third row: the wavenumber power spectra of IDD-mode (e) and LRRC mode (f), respectively.

with previous DIII-D observations [26]. The electron and ion temperature profiles are varied with $T_{e,i} \propto B_r^2$ (Figures 1(c) and (d)), such that the T_e/T_i ratio and the gyro-radii ρ_s are kept nearly constant in the mid-radius region during the scan. The corresponding electron collisionality, ν_e^* , is increased by a factor of 7 in the mid-radius region (Figure 1(b)). The normalized electron and ion temperature gradient, $L_T^{-1} = -\nabla_r \ln T$, are similar during the scan (Figures 1(g) and (h)). The toroidal rotation drops when the collisionality is raised. As a result, the mean $E_r \times B$ shear flow and its shearing rate reduced substantially at higher collisionality (Figures 1(e) and (f)). Here, the $E_r \times B$ mean flow shearing rate, $V'_{E \times B}$, is calculated using the Waltz-Miller formulation [27]. Moreover, the core thermal diffusivity, given by the local power balance analysis using the TRANSP code, increases by a factor of 2–3 at high collisionality (Figures 1(i)). The effective ion thermal diffusivity is only marginally higher in high collisionality shots (Figures 1(j)).

With different levels of collisionality and $E_r \times B$ shear flows, density fluctuations exhibit differing spectral and temporal characteristics. In the high collisionality discharges, with a

weak $E_r \times B$ shear flow, two different modes can be detected by the DBS diagnostics between ELMs (Figure 2(a)). Here, the ELM evolutions are indicated by the D_α emission intensity (gray curves). One mode has a negative Doppler frequency shift corresponding to ion diamagnetic drift direction (IDD) in the lab frame (IDD-mode marked by cyan circles); the other mode has a positive Doppler frequency shift around 2 MHz propagating in the electron diamagnetic drift direction (EDD) in the lab frame (EDD-mode marked by blue circles). In low collisionality discharges, with strong $E_r \times B$ shear flow, the IDD-mode with $f < 0$ can still be observed with a larger Doppler shift, but the EDD-mode around $f \approx 2$ MHz is weak and rarely happened (Figure 2(b)). Note that the scales of both the IDD-mode and EDD-mode are in the sub-ion-gyroradius regime.

In this study, the EDD-mode is of interest as it exhibits a long-radial-range correlation, i.e., a LRRC mode. Figure 2(c) shows the frequency resolved coherence $\gamma^2(f)$ between electron density fluctuations at $\rho \approx 0.4$ and 0.5 . The fluctuations at $f < 0$ do not show any clear coherence between different radial locations, while the LRRC mode at $f \approx 2$ MHz shows substantial coherence with lower mean $E_r \times B$ shear flow. Figure 2(d) shows the radial profiles of the peak coherence for underlying turbulence of the LRRC mode, using the measurements at $\rho \approx 0.4$ as the reference. The radial correlation length can be obtained via the decay length of the exponential fits, i.e., $\gamma^2(\rho) = \gamma^2(\rho_0) \exp(-\frac{\rho - \rho_0}{L_{c,r}})$, where $L_{c,r}$ represents the radial correlation length in terms of the minor radius fraction. The radial correlation length of the LRRC mode, $L_{c,r}$, is no more than 2 cm (plasma minor radius $a \approx 61$ cm) with strong $E_r \times B$ shear flow, while it increases to about 10 cm with reduced $E_r \times B$ shear flow in high collisionality plasmas. This long radial correlation length indicates a radially elongated structure of the LRRC mode, i.e., $k_r \ll k_\theta$ with $k_r \rho_s = 0.1 - 0.3$ and $k_\theta \rho_s = 1 - 4$.

The wavenumber power spectra of electron density fluctuations are displayed in Figures 2(e) and (f). It is found that the wavenumber power spectra of the IDD-mode obey a power-law of $S(k_\perp) \propto k_\perp^{-3}$ and are similar in the magnitude for discharges with low and high $E_r \times B$ shear flows (Figure 2(e)). The negligible variations in magnitude indicate that it is *not* likely responsible for the changes in the plasma confinement during the collisionality scan. On the other hand, the power spectrum of LRRC mode is much larger in the weak $E_r \times B$ shear and high collisionality discharges, and shows a power-law of $S(k_\perp) \propto k_\perp^{-1}$ (Figure 2(f)). The $1/k$ spectrum of the LRRC mode is indicative of its avalanching-like behavior that are commonly associated with self-organized criticality (SOC) [9, 28].

The envelopes of the LRRC mode also show a clear cross-correlation across a wide radial range. As shown in Figure 3(a), the envelopes, or root-mean-square (RMS) levels, of density fluctuations corresponding to the LRRC mode at different radial locations are well aligned in time. Correlation analysis reveals that the cross-correlation coefficient between the envelopes at $\rho \approx 0.4$ and 0.5 approaches the value of one with weak flow

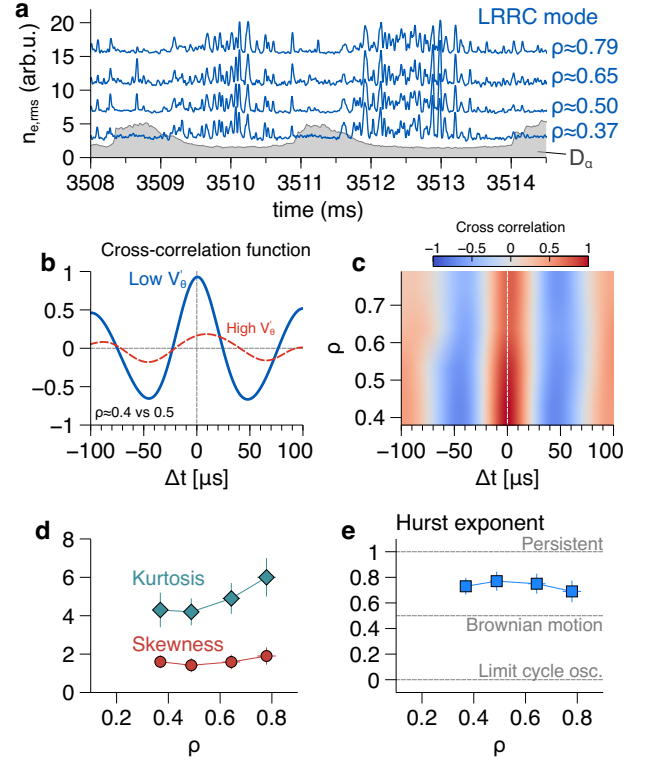


Figure 3. (a) Time evolution of the envelopes (RMS levels) of local density fluctuations (with offsets) corresponding to the LRRC mode at different radial locations. (b) Cross-correlation function between RMS levels at $\rho \approx 0.4$ and 0.5 for two different cases. (c) Contours of the cross correlation function between RMS levels for each DBS channel, with inner most channel as the reference. (d) Skewness and Kurtosis and (e) the Hurst exponent of the underlying fluctuations of LRRC turbulence. The error bars indicates the standard error of the statistical analysis.

shear, while the one in strong flow shear case is insignificant (Figure 3(b)). Note that the amplitude of the LRRC mode reduced substantially in the strong flow case. This value is well below the By plotting the cross-correlation of the envelopes as a function of the radial location and the time lag, for the weak flow case (Figure 3(c)), with inner most channel as the reference, one can see that the envelope of the LRRC mode spans a broad radial range of spatial scales ($\rho_i \ll \Delta r_i^{env} \lesssim a$) with a negligible time delay (no more than a few micro-seconds). Such a wide radial scale of the envelopes of shorter wavelength turbulence indicates the emergence of streamer-like transport events in the weak flow shear discharges.

The statistical analysis of the underlying density fluctuations corresponding to the LRRC mode show large values of skewness ($S = 1 - 2$) and kurtosis ($K = 4 - 6$) (Figure 3(d)), indicative of highly intermittent features of underlying turbulence. The Hurst exponent has been calculated using the technique of rescaled range analysis [29], and is found to range from 0.7 to 0.8 (Figure 3(e)). This Hurst exponent is well above the value of 0.5 that corresponds to the Brownian motion, indicating a long-term memory characteristic in the LRRC mode. Here,

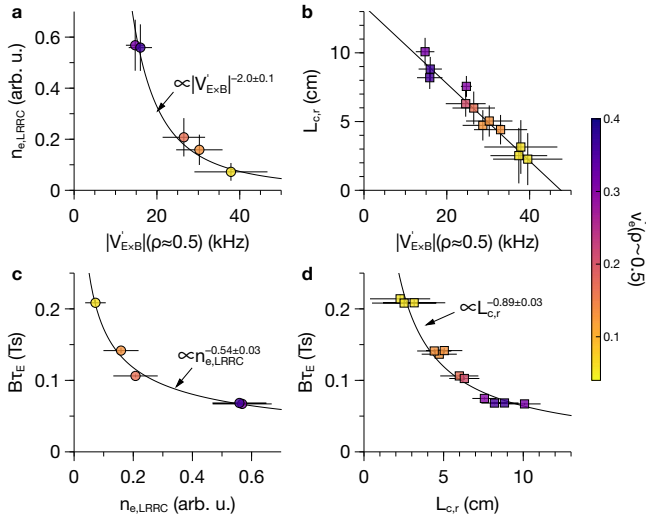


Figure 4. The amplitude (a) and the radial correlation length (b) of the underlying fluctuations of LRRC transport events are plotted against the local $E_r \times B$ velocity shearing rate at $\rho \approx 0.5$. Normalized confinement time is compared against the amplitude RMS levels (c) and the radial correlation length of LRRC turbulence (d), respectively. The collisionality of each discharge at $\rho \approx 0.5$ is color-coded, with brighter markers corresponding to lower collisionality.

the Hurst exponent and higher order moments are calculated for each inter-ELM period, and a total time interval of 200 ms (about 60 samples) is used to estimate the means and standard errors.

To gain further insights into the influence of the $E_r \times B$ shear flow on those LRRC turbulent structures, we compare the amplitude ($k_{\perp} \rho_s \sim 3$) and the radial correlation length of underlying turbulence of LRRC transport events against the local $E_r \times B$ shearing rate at $\rho \approx 0.5$ (Figure 4(a)). The collisionality (at $\rho \approx 0.5$) of each discharge is color-coded, with brighter markers corresponding to lower collisionality discharges. As shown in Figure 4(a), when the local $E_r \times B$ flow shearing rate is increased, the amplitude of the LRRC mode decreases as $\tilde{n}_{e,LRRC} \propto |V'_{E \times B}|^{-2}$. The radial correlation length is inversely correlated to the local $E_r \times B$ shearing rate (Figure 4(b)). For weak flow shear case, the turbulent scattering rate is estimated using the inverse of the eddy turnover time of LRRC mode, i.e., $\tau_c^{-1} \approx 20 - 30$ kHz. Here, the eddy turnover time of LRRC mode is calculated using the auto-correlation time of the corresponding RMS levels at high collisionality and weak flow shear, and thus it is independent of Doppler shifts due to the background mean flow. It is found that the amplitude and radial scale of the LRRC mode increase substantially when $|V'_{E \times B}| < \tau_c^{-1}$ (Figure 4(a) and (b)). This finding is an indication that the mean $E_r \times B$ shear flow impacts the development of the LRRC turbulent structures, consistent with the shear decorrelation mechanism. It is worth noting that the reduced mean shear layer is associated with the high collisionality in this study, and further experiments using net-zero torque input are desirable to distinguish effects

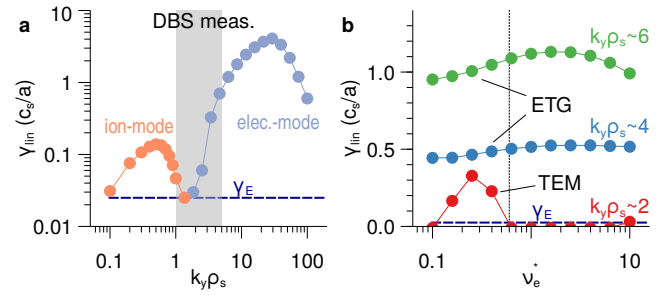


Figure 5. Linear growth rate calculation using CGYRO code for (a) wavenumber scan in high collisionality plasma at $\rho \approx 0.6$ and (b) collisionality scan at three different wavenumbers. The black dashed line in (b) indicates the experiment value of local collisionality.

of collisionality and mean shear flows.

The development of LRRC turbulent structures and the resulting transport events is also associated with degradation of the normalized confinement time (Figure 4(c) and (d)), which is in conformity with previous results that the plasma transport increases with collisionality in H -mode plasmas [18]. In particular, the dependence on the LRRC mode amplitude, $B\tau_E \sim |\tilde{n}_{e,LRRC}|^{-0.54 \pm 0.03}$, appears to be close to the collisionality scaling, $B\tau_E \sim \nu_*^{-0.56 \pm 0.06}$, previously reported on DIII-D [17]. Note that enhanced turbulent transport here is not likely driven by ion-scale long-wavelength turbulence ($k_{\theta} \rho_s < 1$) which is reported to slightly decrease in the core when collisionality is raised by a factor of 5 [26]. Also, nonlinear gyro-kinetic simulations show that the calculated ion-scale turbulent transport underestimates the total electron heat flux by an order of magnitude, particularly in high collisionality plasmas [30], implying the essential role of the higher- k_{θ} turbulence ($k_{\theta} \rho_s > 1$) in electron transport processes at high collisionality. These findings suggest that the emergence of LRRC transport events may serve as a candidate explanation for confinement degradation in DIII-D H -mode fusion plasmas at higher collisionality [17, 18].

Linear gyrokinetic simulations have been performed to identify the underlying turbulence of those LRRC transport events using the CGYRO code. It is found that electrostatic instabilities with $k_{\theta} \rho_s > 2$ are linearly unstable (Figure 5(a)). Two common instabilities in this range are the trapped electron mode (TEM) and the electron temperature gradient mode (ETG). The TEM is found to be linearly stabilized in high collisionality plasmas in this study, via a collisionality scan (red in Figure 5(b)), so it is unlikely responsible for the long-radial-range-correlation transport events. The ETG mode, on the other hand, is still linearly unstable at higher collisionality according to the gyrokinetic simulation (green and blue Figure 5(b)). Previous nonlinear gyrokinetic simulations suggest ETG mode can lead to streamer-like transport events [11, 30, 31], which seems to agree with the observations in this study.

In summary, the shorter wavelength ($1 < k_{\theta} \rho_s < 4$) core turbulence can develop into long-radial-range correlated turbulent structures in high-collisionality H -mode plasmas with reduced

mean $V_{E \times B}$ shear flow on the DIII-D tokamak. These turbulent structures are radially elongated, and their envelopes span a wide range in the mid-radius region, leading to streamer-like transport events. The underlying turbulence shows statistical features that are usually associated with self-organized criticality, including intermittency (large skewness and kurtosis), long-term memory effect (large Hurst exponent), and characteristic power spectrum ($S(k_{\perp}) \propto k^{-1}$). The amplitude and the radial scale of the turbulent structures increase substantially once the mean flow shearing rate is decreased below the turbulent scattering rate. The observations summarized here constitute the first experimental demonstration of the nonlocal turbulent transport events in high-confinement fusion plasmas, and also provide evidence for the role of $V_{E \times B}$ shear flow in regulating the long-range correlated turbulent structures.

The authors greatly appreciate the effort and support of the entire DIII-D team in performing these experiments. We would like to acknowledge valuable discussions with M. E. Austin, N. A. Crocker, and G. R. McKee. This material is based upon work supported by the U.S. Department of Energy, Office of Science, Office of Fusion Energy Sciences, using the DIII-D National Fusion Facility, a DOE Office of Science user facility, under Awards DE-FC02-04ER54698 and DE-SC0019352.

Disclaimer: This report was prepared as an account of work sponsored by an agency of the United States Government. Neither the United States Government nor any agency thereof, nor any of their employees, makes any warranty, express or implied, or assumes any legal liability or responsibility for the accuracy, completeness, or usefulness of any information, apparatus, product, or process disclosed, or represents that its use would not infringe privately owned rights. Reference herein to any specific commercial product, process, or service by trade name, trademark, manufacturer, or otherwise does not necessarily constitute or imply its endorsement, recommendation, or favoring by the United States Government or any agency thereof. The views and opinions of authors expressed herein do not necessarily state or reflect those of the United States Government or any agency thereof.

-
- [1] B. Hof, C. W. H. v. Doorne, J. Westerweel, F. T. M. Nieuwstadt, H. Faisst, B. Eckhardt, H. Wedin, R. R. Kerswell, and F. Waleffe, *Science* **10.1126/science.1100393** (2004), publisher: American Association for the Advancement of Science.
- [2] T. Yamada, S.-I. Itoh, T. Maruta, N. Kasuya, Y. Nagashima, S. Shinohara, K. Terasaka, M. Yagi, S. Inagaki, Y. Kawai, A. Fujisawa, and K. Itoh, *Nature Physics* **4**, 721 (2008).
- [3] C. Bédard, H. Kröger, and A. Destexhe, *Physical Review Letters* **97**, 118102 (2006), publisher: American Physical Society.
- [4] R. Albert and A.-L. Barabási, *Reviews of Modern Physics* **74**, 47 (2002), publisher: American Physical Society.
- [5] C.-L. Hung, X. Zhang, N. Gemelke, and C. Chin, *Nature* **470**, 236 (2011).
- [6] E. J. Doyle, W. A. Houlberg, Y. Kamada, V. Mukhovatov, T. H. Osborne, A. Polevoi, G. Bateman, J. W. Connor, J. G. Cordey, T. Fujita, X. Garbet, T. S. Hahm, L. D. Horton, A. E. Hubbard, F. Imbeaux, F. Jenko, J. E. Kinsey, Y. Kishimoto, J. Li, T. C. Luce, Y. Martin, M. Ossipenko, V. Parail, A. Peeters, T. L. Rhodes, J. E. Rice, C. M. Roach, V. Rozhansky, F. Ryter, G. Saibene, R. Sartori, A. C. C. Sips, J. A. Snipes, M. Sugihara, E. J. Synakowski, H. Takenaga, T. Takizuka, K. Thomsen, M. R. Wade, and H. R. Wilson, *Nuclear Fusion* **47**, S18 (2007).
- [7] K. Ida, Z. Shi, H. J. Sun, S. Inagaki, K. Kamiya, J. E. Rice, N. Tamura, P. H. Diamond, G. Dif-Pradalier, X. L. Zou, K. Itoh, S. Sugita, O. D. Gürcan, T. Estrada, C. Hidalgo, T. S. Hahm, A. Field, X. T. Ding, Y. Sakamoto, S. Oldenbürger, M. Yoshinuma, T. Kobayashi, M. Jiang, S. H. Hahn, Y. M. Jeon, S. H. Hong, Y. Kosuga, J. Dong, and S.-I. Itoh, *Nuclear Fusion* **55**, 013022 (2015).
- [8] T. S. Hahm and P. H. Diamond, *Journal of the Korean Physical Society* **73**, 747 (2018).
- [9] P. H. Diamond and T. S. Hahm, *Physics of Plasmas* **2**, 3640 (1995), publisher: American Institute of Physics.
- [10] T. S. Hahm, P. H. Diamond, Z. Lin, K. Itoh, and S.-I. Itoh, *Plasma Physics and Controlled Fusion* **46**, A323 (2004), publisher: IOP Publishing.
- [11] W. Dorland, F. Jenko, M. Kotschenreuther, and B. N. Rogers, *Physical Review Letters* **85**, 5579 (2000), publisher: American Physical Society.
- [12] K. W. Gentle, W. L. Rowan, R. V. Bravenec, G. Cima, T. P. Crowley, H. Gasquet, G. A. Hallock, J. Heard, A. Ouroua, P. E. Phillips, D. W. Ross, P. M. Schoch, and C. Watts, *Physical Review Letters* **74**, 3620 (1995), publisher: American Physical Society.
- [13] R. Nazikian, K. Shinohara, G. J. Kramer, E. Valeo, K. Hill, T. S. Hahm, G. Rewoldt, S. Ide, Y. Koide, Y. Oyama, H. Shirai, and W. Tang, *Physical Review Letters* **94**, 135002 (2005).
- [14] Y. Hamada, T. Watari, A. Nishizawa, K. Narihara, Y. Kawasumi, T. Ido, M. Kojima, and K. Toi, *Physical Review Letters* **96**, 115003 (2006).
- [15] S. Inagaki, T. Tokuzawa, K. Itoh, K. Ida, S.-I. Itoh, N. Tamura, S. Sakakibara, N. Kasuya, A. Fujisawa, S. Kubo, T. Shimozuma, T. Ido, S. Nishimura, H. Arakawa, T. Kobayashi, K. Tanaka, Y. Nagayama, K. Kawahata, S. Sudo, H. Yamada, and A. Komori, *Physical Review Letters* **107**, 115001 (2011).
- [16] X. Q. Ji, Y. Xu, C. Hidalgo, P. H. Diamond, Y. Liu, O. Pan, Z. B. Shi, and D. L. Yu, *Scientific Reports* **6**, 32697 (2016).
- [17] T. C. Luce, C. C. Petty, and J. G. Cordey, *Plasma Physics and Controlled Fusion* **50**, 043001 (2008).
- [18] C. C. Petty and T. C. Luce, *Physics of Plasmas* **6**, 909 (1999), publisher: American Institute of Physics.
- [19] S. M. Kaye, F. M. Levinton, D. Stutman, K. Tritz, H. Yuh, M. G. Bell, R. E. Bell, C. W. Domier, D. Gates, W. Horton, J. Kim, B. P. LeBlanc, N. C. Luhmann, R. Maingi, E. Mazzucato, J. E. Menard, D. Mikkelsen, D. Mueller, H. Park, G. Rewoldt, S. A. Sabbagh, D. R. Smith, and W. Wang, *Nuclear Fusion* **47**, 499 (2007), publisher: IOP Publishing.
- [20] M. Valovic, R. Akers, M. d. Bock, J. McCone, L. Garzotti, C. Michael, G. Naylor, A. Patel, C. M. Roach, R. Scannell, M. Turnyanskiy, M. Wisse, W. Guttenfelder, and J. C. and, *Nuclear Fusion* **51**, 073045 (2011), publisher: IOP Publishing.
- [21] J. L. Luxon, *Nuclear Fusion* **42**, 614 (2002), publisher: IOP Publishing.
- [22] D. Eldon, B. D. Bray, T. M. Deterly, C. Liu, M. Watkins, R. J. Groebner, A. W. Leonard, T. H. Osborne, P. B. Snyder, R. L. Boivin, and G. R. Tynan, *Review of Scientific Instruments* **83**, 10E343 (2012), publisher: American Institute of Physics.
- [23] C. Chrystal, K. H. Burrell, B. A. Grierson, S. R. Haskey, R. J. Groebner, D. H. Kaplan, and A. Briesemeister, *Review of Scientific Instruments* **87**, 11E512 (2016), publisher: American Institute of Physics.

- [24] K. H. Burrell, [Physics of Plasmas](#) **4**, 1499 (1997).
- [25] W. A. Peebles, T. L. Rhodes, J. C. Hillesheim, L. Zeng, and C. Wannberg, [Review of Scientific Instruments](#) **81**, 10D902 (2010).
- [26] S. Mordijck, T. L. Rhodes, L. Zeng, A. Salmi, T. Tala, C. C. Petty, G. R. McKee, R. Reksoatmodjo, F. Eriksson, E. Fransson, and H. Nordman, [Nuclear Fusion](#) **60**, 066019 (2020), publisher: IOP Publishing.
- [27] R. E. Waltz and R. L. Miller, [Physics of Plasmas](#) **6**, 4265 (1999), publisher: American Institute of Physics.
- [28] P. Bak, C. Tang, and K. Wiesenfeld, [Physical Review Letters](#) **59**, 381 (1987).
- [29] M. Gilmore, C. X. Yu, T. L. Rhodes, and W. A. Peebles, [Physics of Plasmas](#) **9**, 1312 (2002).
- [30] C. Holland, N. T. Howard, and B. A. Grierson, [Nuclear Fusion](#) **57**, 066043 (2017), publisher: IOP Publishing.
- [31] F. Jenko and W. Dorland, [Physical Review Letters](#) **89**, 225001 (2002), publisher: American Physical Society.